DETAILED ANALYSIS OF A GEOEFFECTIVE ICME TRIGGERED BY THE MARCH 15, 2013 CME

DIANA BEŞLIU-IONESCU[1], GEORGETA MARIŞ MUNTEAN[1],
DANIELA A. LĂCĂTUŞ[1], ALIN R. PARASCHIV[1], MARILENA MIERLA[2,1]

[1] *"Sabba S. Ştefănescu" Institute of Geodynamics of the Romanian Academy, 19–21, Jean-Louis Calderon St., 020032 Bucharest, Romania, diana.ionescu@geodin.ro*
[2] *Royal Observatory of Belgium, Ringlaan 3, 1180 Brussels, Belgium*

We present in this paper a detailed analysis of a coronal mass ejection (CME) that was registered on March 15, 2013 in LASCO-C2 images. It propagated into the interplanetary space towards the Earth and it was followed by a geomagnetic storm defined by a minimum Dst = -132 nT on March 17, 2013. We apply the forward model (Thernisien *et al.*, 2006) to compute the real speed and direction of propagation. We apply a modified version of the regression model (Srivastava, 2005) to compute the probability that this CME will trigger a super-intense geomagnetic storm and we found a 100% probability to have an intense storm with a minimum Dst value between -150 nT and -200 nT. This probability is not in accordance with the observations and we believe that to be a direct consequence of the small data-base our model was trained on.

Key words: geomagnetic storm, CME, ICME.

1. INTRODUCTION

Coronal mass ejections (CMEs) are huge explosions of magnetised plasma from the Sun into the interplanetary medium. When observed into the interplanetary space they are called interplanetary coronal mass ejections (ICMEs). It has been established that CMEs are the primary source of major geomagnetic storms (Gosling, 1993; Gopalswamy *et al.*, 2004; Zhang *et al.*, 2007).

Gonzalez *et al.* (1994) defined a geomagnetic storm as "an interval of time when a sufficiently intense and long lasting interplanetary electric field leads, through a substantial energization in the magnetosphere-ionosphere system, to an intensified ring current strong enough to exceed some key threshold of the quantifying storm time Dst (Disturbance Storm Time) index". Geomagnetic storms can have serious consequences over our life by means of electric power and telecommunications related problems.

Other phenomena that may trigger a geomagnetic storm are the High Speed Streams (HSS). The HSS are coming from coronal holes and have average speeds around 700 km/s (see *e.g.* Intriligator, 1973, 1974; Gosling *et al.*, 1976, Iucci *et al.*, 1979). For further details (such as differentiating streams, alternate definitions and catalogues) please read the "High Speed Streams in the Solar Wind in Solar Cycle 24" by Georgeta Mariş Muntean *et al.* (2014, in print).

The geomagnetic storms are measured via geomagnetic indices: aa, Dst, AE, AP, Kp. These indices are currently provided by the Geomagnetic World Data Centre at Kyoto. Depending on the value of the geomagnetic index there are four different classes of geomagnetic storm defined as a function of the Dst index: substorms or minor storm (-50 nT < Dst < -30 nT), moderate storms (-100 nT < Dst < -50 nT), intense (-150 < Dst < -100 nT) and super-intense or major storms (Dst < -150 nT). The consequences of severe storms can be very destructive such as: satellite malfunctions, voltage control problems, low-frequency radio navigation disruptions etc. Thus the investigation of possible links between various geoeffective phenomena is of great importance.

This paper focuses on analysing in detail the consequences of the ICME registered on March 17, 2013 at ACE and followed by a geomagnetic storm with minimum Dst = -132 nT and its associated CME from March 15, 2013.

2. DATA DESCRIPTION

We have identified geomagnetic storms using the online data available at the World Data Center for Geomagnetism, Kyoto (wdc.kugi.kyoto-u.ac.jp/) and chose an event from March 17, 2013 because of its interesting evolution and its connection to an ICME. We have used the Richardson and Cane catalogue (Richardson and Cane, 2010) to identify the ICME. This catalogue is available online at: srl.caltech.edu/ACE/ASC/DATA/level3/icmetable2.htm.

The CME associated with this event is a full halo one, registered by LASCO (Brueckner *et al.*, 1995) on March 15, 2013 at 07:12 UT (see the manual CME catalogue at cdaw.gsfc. nasa. gov/CME_list/ or the automatic catalogue at sidc.oma.be/cactus/). The CME was also observed by the COR2 coronagraphs (Howard *et al.*, 2008) onboard STEREO (Kaiser *et al.*, 2008). The two STEREO missions were separated by 87 degrees at the time of the observations (with STEREO-A 132 degrees ahead the Earth and STEREO-B 141 degrees behind the Earth).

See also the SIDC bulletins at sidc.be/archive for the complete CME – ICME – geomagnetic storm chain prediction.

2.1. THE CME

On March 15, 2013 a full halo CME was registered by LASCO onboard SOHO at 07:12:05 UT. It had a linear projected speed of 1063 km/s and a projected speed of 1247 km/s at the final height of 27 solar radii (see on line CME catalogue). Fig. 1 shows running-differences of LASCO-C2 coronograph white-light images where the evolution in time and space of this CME is very distinctive. The previous image in time was subtracted from the current frame in order to outline the outer moving features. The bright feature in the images is plasma moving outwards and the dark feature is the plasma from the previous frame which was subtracted in the current frame.

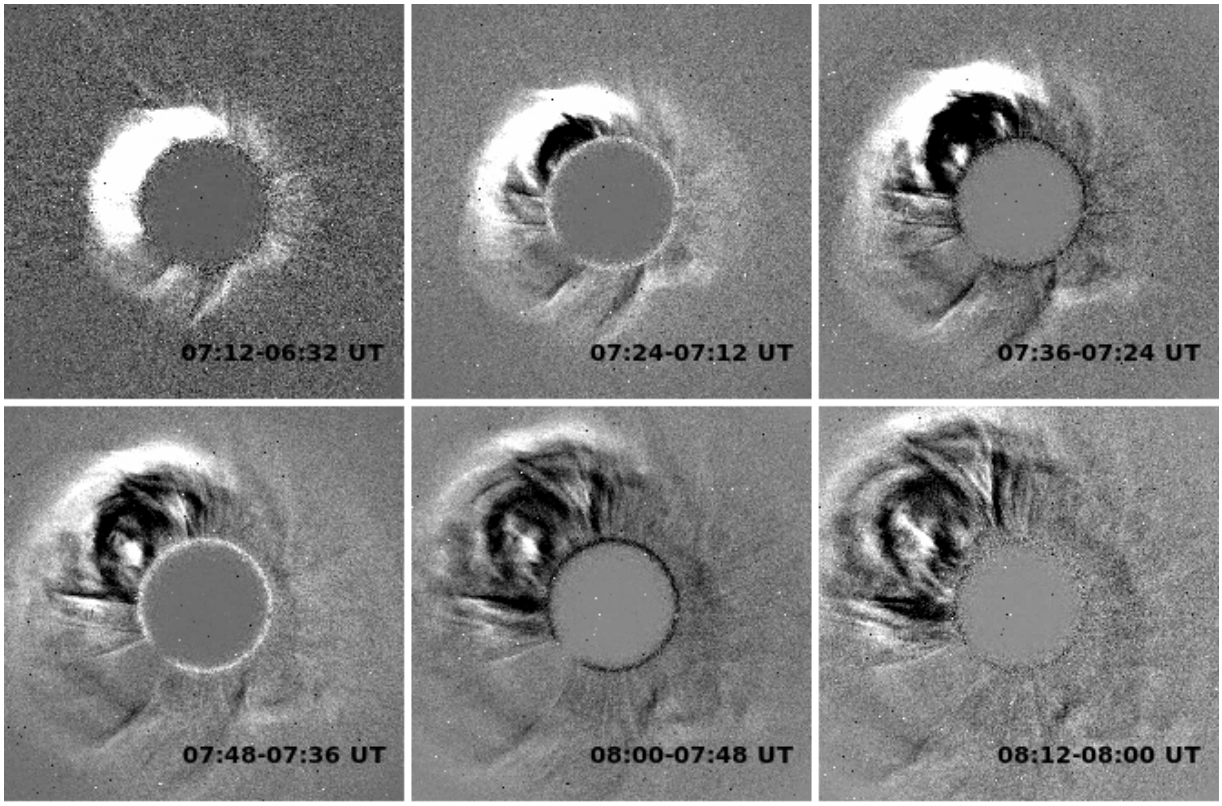

Fig. 1 – Running-differences of LASCO-C2 white-light images for the CME on March 15, 2013.

The CME was also observed by COR2-A at around 06:39 UT as a full halo and by COR2-B at around 06:54 UT as a partial halo. It was a backside event as observed by STEREO.

This CME event as many other that produced major geomagnetic storms (*e.g.*, Halloween Events of 2003, Nov 15, 2007 event, etc.) is associated with a solar flare. It was an X-ray solar flare of class M1.1 coming from AR 11692 which had an α-magnetic configuration and it was located at N09E05. This is not a very powerful flare, but it was a very long one. It started at 05:46 UT, peaked at 06:58 UT and ended at 08:35 UT. The CME followed a short time (~14 minutes) after the maximum X-ray emission of the flare.

2.2. THE ICME

The shock of the ICME associated with March 15, 2013 full halo CME was registered at ACE on March 17, 06:00 UT and the plasma field started at 15:00 UT and ended two days later at 16:00 UT. The increase in speed was 230 km/s, the mean speed during the ICME was 520 km/s, while the maximum speed was 720 km/s. The transit speed at 1 AU was 890 km/s. The transit speed was calculated as the ratio between the distance Sun – spacecraft and the time the CME took to arrive at the spacecraft. B was 9.5 nT, Bz -0.7 nT with a minimum value of -14.4 nT at 09:00 on March, 17.

Fig. 2 shows various parameters characterising the ICME. The first four rows show the interplanetary magnetic field, components – Bx, By, Bz – and the total magnetic field intensity (B). The vertical line shows the arrival time of the shock at Earth. The vertical dashed lines represent the start and the end of the ICME based primarily on plasma and magnetic field observations (Richardson and Cane, 2003). The dash-dot vertical line represents the moment that minimum Dst value was reached. The storm is described in the next session.

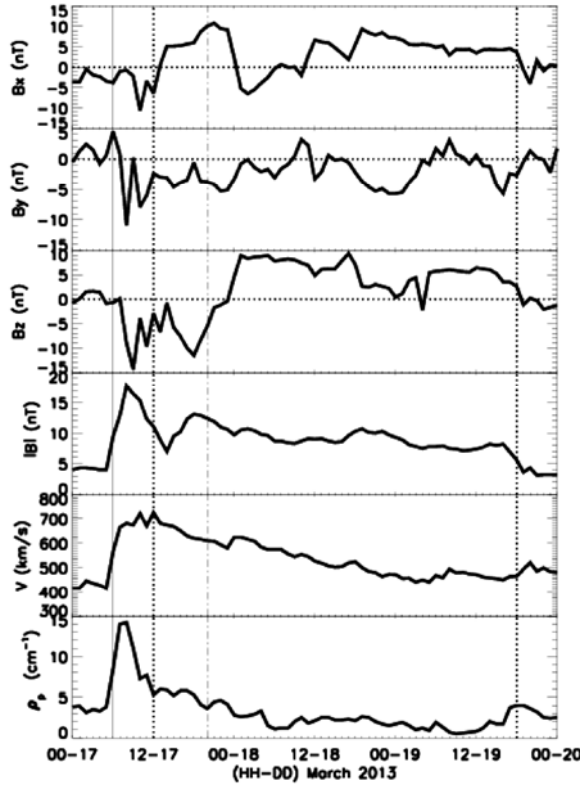

Fig. 2 – ICME parameters evolution during 17-20 March: (from top row to bottom row) Bx, By, Bz and scalar B in GSM coordinates, plasma velocity and proton density. Vertical line shows arrival time of the shock at Earth. Vertical dash-dotted shows the minimum Dst time. Vertical dotted line shows the beginning and end of the ICME.

2.3. THE GEOMAGNETIC STORM

On March 17 at 6:00 the Dst registered a single positive value after which, in 13 hours, the Dst reached its minimum value of -132 nT, as seen in Fig. 3. This defines an intense geomagnetic storm.

In just three hours the Dst index suddenly dropped to -89 nT. For almost seven hours its values oscillate around -85 nT. After just three more hours the Dst reached its minimum value of -132 nT at 20:00 UT.

After 22:00 UT the Dst values tend to come back to previous storm levels, but due to another ICME superposition they do not recover above -42 nT.

This is a typical sudden storm commencement behaviour, with all three characteristic phases: beginning, main and recovering phase well defined, but is has a step like limit in those seven hours between 10:00 and 17:00 UT.

The SSC in Dst is accompanied by a peak in the AE index of about 10 times the quiet level. The AE maximum is reached 4 hours earlier than the minimum value of Dst.

All three components of the interplanetary magnetic field are rotating during the main phase of the geomagnetic storm (see Fig. 2). The southward component remains negative during the entire storm. During the recovery phase Bx and Bz still oscillate for a while, but towards the end of the ICME they show a more steady behaviour. The time that Bz heavily oscillates coincides with the period of flattening of the Dst.

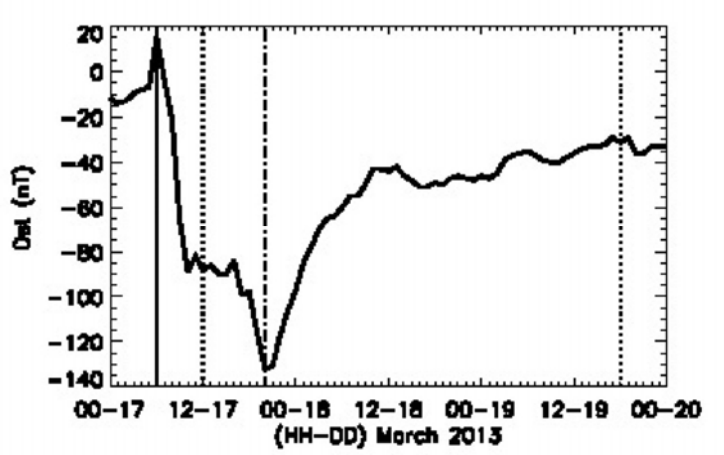

Fig. 3 – Dst temporal profile between March 17 and 20, 2013
The vertical lines same as Fig. 2.

After the main phase of the storm, Bz remains negative for about five hours and returns to positive values. The end of the ICME is not extremely clear, because starting March 20 there is another ICME hitting the magnetosphere.

The magnitude of the solar wind speed (fourth row in Fig. 2) suddenly increases from 400 km/s to ~750 km/s during the main phase of the storm. It has a local minimum around 14:00 UT then has another peak at the time the minimum value of the Dst is reached.

The last row in Fig. 2 shows the proton density, which increases by a factor of four in the first two hours of the main phase, then steadily decreases to pre-storm levels.

Table 1 shows the summary of the events described above.

3. DATA ANALYSIS

3.1. 3D RECONSTRUCTION OF THE CME

We reconstructed the 3D structure of the CME, using a forward modelling technique (Thernisien *et al.*, 2006), in order to infer the propagation direction and the real speed of the CME. The geometrical model resembles a flux-rope like CME. It consists of a section shaped as a tube forming the main body of the structure

attached to two cones that correspond to the "legs" of the CME. The shape resembles the reminiscent of a croissant. The parameters of this model are changed until best fit the observations.

The method can reproduce the large scale structure of the CME, but it does not give any information about the internal structure. Before applying the model, the COR2 polarised images were processed using the Solar Soft routine secchi_prep.pro in order to obtain total brightness images. Then the frame prior to the first appearance of the CME in COR2 field of view (FOV) was subtracted from the frames where the CME was observed. In this way we eliminated the emission from stable structures (such as streamers) and the unwanted emission from the stray-light, noise, etc. The information left was only the emission from the dynamical event (the CME in our case). We fit the CME outline on these images by varying a set of eight parameters characterising the model (longitude, latitude, radius, tilt angle, ratio and half angle) on all of the frames containing the CME. Knowing the time step between the images and the evolution of height in time, the real speed can be easily derived.

Table 1

Various parameters specific to the CME (Date and time, projected speed (km/s) at 27 solar radii, acceleration, the solar source location N09W05), to the ICME (disturbance date and time, start and end of the ICME, the maximum and mean speed, the transit speed in km/s) and the GS (the minimum Dst value (in nT) and the date and time when this value was reached)

CME				ICME					GS	
Date/ Time	V_{proj}	Acc.	Solar Source Location	Shock	Start- End	V_{max}	V_{mean}	V_{tranz}	Dst_{min}	Dst_{min} Date/ Time
15.03/ 07:12	1247	25.8	N09E05	17.03 15:00	17.03/15:00– 19.03/16:00	720	520	890	-132	17.03/ 20:00

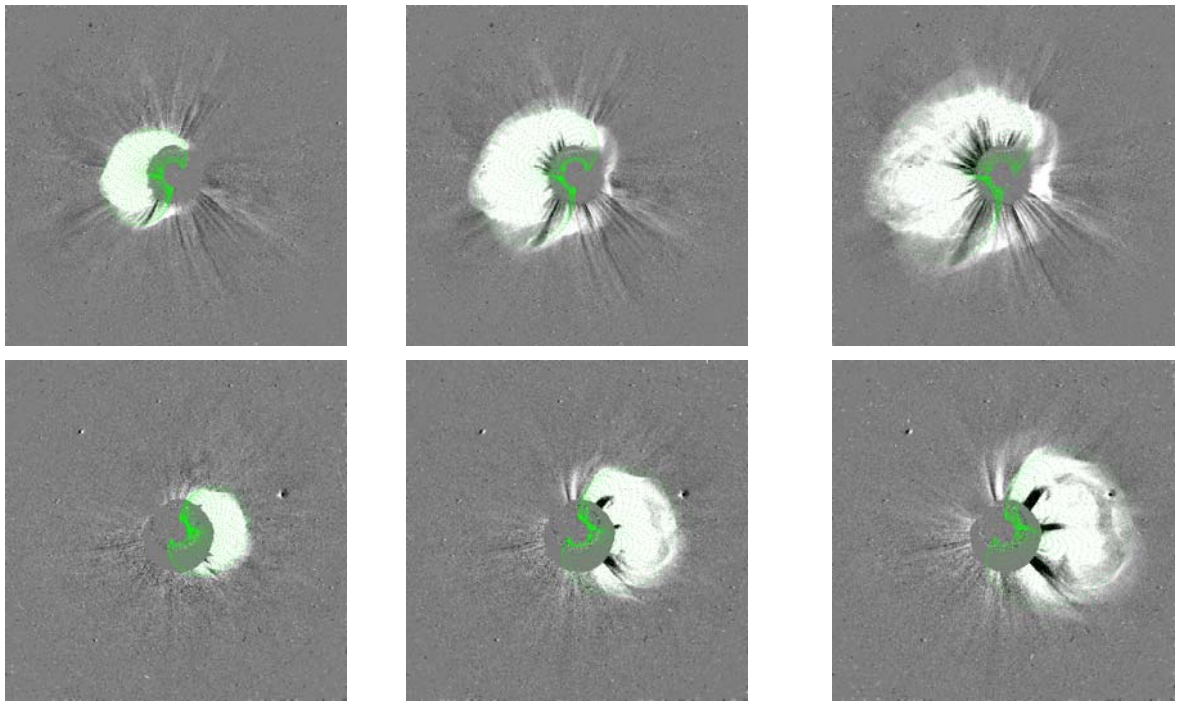

Fig. 4 – The Forward model applied to the March 15, 2013 CME. First row images from STEREO-A. Second row images from STEREO-B. Column times: 07:24 UT, 07:54 UT and 08:24 UT respectively. Over-plotted contours show the flux rope model of the CME.

Table 2

The parameters derived from applying the forward modelling on the CME of March 15, 2013

Date	Time (COR2)	Lon	Lat	Tilt angle	Height R_{Sun}	Ratio	Half angle	Speed (km/s)	Goodness of the fit (A+B) (%)
15.03.2013	07.24	9	-10	-61	8.35	0.61	44	1144	83.37
15.03.2013	07.54	8	-7	-61	10.83	0.61	55		80.53
15.03.2013	08.24	10	-6	-61	14.27	0.61	51		74.38

Fig. 4 shows a sequence of the images on which the forward modelling was applied. On the top row there are the images from STEREO-A, on the bottom row the images from STEREO-B. Each column is a specific time, respectively: 07:24 UT, 07:54 UT and 08:24 UT.

The 3D parameters derived from forward modelling are shown in Table 2.

We see that the 3D speed (1144 km/s) is slightly lower than the projected speed measured in LASCO at 27 solar radii (1247 km/s). Note that the 3D speed is measured at heights less than 15 solar radii, where the projected speed measured in LASCO is around 1100 km/s (*i.e.* very similar with the 3D speed). In this case, LASCO measured the projected expansion speed of the CME, while the 3D speed is the radial speed of the nose of the CME. When comparing the derived latitude and longitude with the source region (N09E05) we notice the deflection towards the south by about 15 degrees. No noticeable deflection in longitude is observed.

As seen from Table 1, the time taken by the CME to reach the ACE spacecraft (which is at Lagrangian point L1) was 47 h. If the CME will travel this distance with the speed calculated from 3D reconstruction, it will take 36 hours. Therefore, the CME has been decelerated into the interplanetary space.

3.2. PROBABILITY OF HAVING A SUPER-INTENSE GEOMAGNETIC STORM

Srivastava (2005) implemented a logistic regression model to predict the occurrence of intense/super-intense geomagnetic storms defined as a highly-simplified, numeric representation of the relation between solar and interplanetary variables and the occurrence of geomagnetic storms.

The author has used seven independent variables (CME/ICME and eruptive phenomena-related coefficients) such as: whether or not the CME was halo, its location, its association with flares, its initial speed, the Southward interplanetary magnetic field (IMF), the total IMF and the ram pressure. The dependent variable was chosen to be the Dst index.

We have increased the number of independent variables to 9, by including the magnetic classification of the active region associated with the CME and the neutral line orientation.

The model equation used was:

$$\Pi_i = \frac{1}{1+e^{-zi}},$$

where $Z_i = b_0 + b_1 \times x_{i1} + ... + b_j \times x_{ij}$

where, Π_i is the probability of the occurrence of major geomagnetic storm given by the i-th observation of the solar variable; b_j ($j = 0$ to J) are model parameters (regression coefficients) x_{ij} ($I = 0$ to I; $j = 0$ to J) are the independent variables; I and J are total number of observations.

We have used the model for 25 ICMEs in SC23 which have produced super-intense geomagnetic storms (Dst < -150 nT), but divided the set into two classes: -200 nT < Dst < -150 nT, respectively Dst < -200 nT. We have trained the model with 21 events, and used the remaining 4 for validation. We obtained a 100% correct prediction for intense storms and 67% successful prediction for super-intense storms.

The probability of this CME to produce a super-intense geomagnetic storm is 1, while the minimum Dst was only -132 nT. It means that the model failed in this case. It is a good indication of the fact that the model needs to be trained on a larger data-base of geomagnetic storms, including intense and minor storms.

4. SUMMARY

We have presented here a detailed analysis of the chain CME–ICME – geomagnetic storm on March 15–17, 2013. We calculated the real speed of the CME by applying a forward modelling on the CME data recorded by COR2 onboard STEREO spacecraft. The speed derived from here is similar to the projected expansion speed measured in LASCO data. The results show that the CME was decelerated into the interplanetary space. Using a modified version of the regression model of Srivastava (2005) we have obtained a 100% probability that the March 15, full halo CME should have produced a super-intense storm. This did not happen and we believe that to be a consequence of the restrictive data-base of geomagnetic storms the model was build on and that it does not count for the magnetic configuration during the CME.

We plan to extend the model to a bigger data set and to improve the prediction.

Acknowledgments. This research was supported from the CNCSIS project IDEI, No. 93/5.10.2011.

We acknowledge the use of SOHO, STEREO, ACE and geomagnetic data. We thank Luciano Rodrigues for useful discussions on ICME magnetic field orientation.

REFERENCES

ANDREWS, M.D. (2003), *A Search for CMEs Associated with Big Flares,* Solar Physics, **218** (1), 261–279.

BRUECKNER, G.E., HOWARD, R.A., KOOMEN, M.J., KORENDYKE, C.M., MICHELS, D.J., MOSES, J.D., SOCKER, D.G., DERE, K.P., LAMY, P.L., LLEBARIA, A., BOUT, M.V., SCHWENN, R., SIMNETT, G.M., BEDFORD, D.K., EYLES, C.J. (1995), *The Large Angle Spectroscopic Coronagraph (LASCO)*, Solar Physics, **162**, (1–2), 357–402.

CANE, H.V., RICHARDSON, I.G. (2003), *Interplanetary coronal mass ejections in the near-Earth solar wind during 1996–2002*, Journal of Geophysical Research (Space Physics), **108** (A4), 1156.

GONZALEZ, W.D., JOSELYN, J.A., KAMIDE, Y., KROEHL, H.W., ROSTOKER, G., TSURUTANI, B.T., VASYLIUNAS, V.M. (1994), *What is a geomagnetic storm?*, **99** (A4), 5771–5792.

GOPALSWAMY, N. (2008), *Solar connections of geoeffective magnetic structures*, Journal of Atmospheric and Solar-Terrestrial Physics, **70** (17), 2078–2100.

GOPALSWAMY, N., YASHIRO, S., AKIYAMA, S. (2007), *Geoeffectiveness of halo coronal mass ejections*, Journal of Geophysical Research (Space Physics), **112** (A6), A06112.

GOPALSWAMY, N., AKIYAMA, S., YASHIRO, S., MICHALEK, G., LEPPINGA, R.P. (2008), *Solar sources and geospace consequences of interplanetary magnetic clouds observed during solar cycle 23*, Journal of Atmospheric and Solar-Terrestrial Physics, **70** (2–4), 245–253.

GOSLING, J.T. (1990), *Coronal mass ejections and magnetic flux ropes in interplanetary space*, Physics of magnetic flux ropes (A92-31201 12-75), 343–364.

GOSLING, J.T., HILDNER, E., MACQUEEN, R.M., MUNRO, R.H., POLAND, A.I., ROSS, C.L. (1976), *The speeds of coronal mass ejection events*, Solar Physics, **48**, 389–397.

HOWARD, R.A., MOSES, J.D., VOURLIDAS, A., NEWMARK, J.S., SOCKER, D.G., PLUNKETT, S.P., KORENDYKE, C.M., COOK, J.W., HURLEY, A., DAVILA, J.M., *et al.* (2008), S*un Earth Connection Coronal and Heliospheric Investigation (SECCHI)*, Space Science Revue, **136**, 67–115.

INTRILIGATOR, D.S. (1973), *Solar Geophysical Data*, Report UAG-27.

INTRILIGATOR, D.S. (1974), *Evidence of Solar-Cycle Variations in the Solar Wind*, Astrophysical Journal, **188**, L23–L26.

IUCCI, N., PARISI, M., STORINI, M., VILLORESI, G. (1979), *High-speed solar-wind streams and galactic cosmic-ray modulation*, Nuovo Cimento C, **2C**, 421–438.

KAISER, M.L., KUCERA, T.A., DAVILA, J.M., ST. CYR, O.C., GUHATHAKURTA, M., CHRISTIAN, E. (2008), *The STEREO Mission: An Introduction*, Space Science Reviews, **136** (1–4), 5–16.

MARIŞ MUNTEAN, G., PARASCHIV, A.R., LĂCĂTUŞ, D., BEŞLIU-IONESCU, D., MIERLA, M. (2014, in print), *High Speed Streams in the Solar Wind during Solar Cycle 24*, Rev. roum. Géophys., **58**, .

RICHARDSON, I.G., CANE, H.V. (2010), *Near-Earth Interplanetary Coronal Mass Ejections during Solar Cycle 23 (1996–2009): Catalog and Summary of Properties*, Solar Physics, **264** (1), 189–237.

SRIVASTAVA, N. (2005), *A logistic regression model for predicting the occurrence of intense geomagnetic storms*, Annales Geophysicae, **23** (9), 2969–2974.

SRIVASTAVA, N., VENKATAKRISHNAN, P. (2004), *Solar and interplanetary sources of major geomagnetic storms during 1996–2002*, Journal of Geophysical Research (Space Physics), **109** (A10), A10103.

THERNISIEN, A.F.R., HOWARD, R.A., VOURLIDAS, A. (2006), *Modeling of Flux Rope Coronal Mass Ejections,* The Astrophysical Journal, **652** (1), 763–773.

ZHANG, J., RICHARDSON, I.G., WEBB, D.F., GOPALSWAMY, N., HUTTUNEN, E., KASPER, J.C., NITTA, N.V., POOMVISES, W., THOMPSON, B.J., WU, C.-C., YASHIRO, S., ZHUKOV, A.N. (2007), *Solar and interplanetary sources of major geomagnetic storms (Dst <= -100 nT) during 1996–2005,* Journal of Geophysical Research (Space Physics), **112** (A12), A10102.

ZHAO, X.P., WEBB, D.F. (2003), *Source regions and storm effectiveness of frontside full halo coronal mass ejections*, Journal of Geophysical Research Space Physics, **108** (A6), SSH 4-1.

Received: September 29, 2013
Accepted for publication: November 6, 2013